Scientific Research Publishing

Open Journal of Metal, 2021, 11, 21-35
https://www.scirp.org/journal/ojmetal
ISSN Online: 2164-277X
ISSN Print: 2164-2761

Effect of Cast Thickness and Austenitizing Temperature on Microstructure and Mechanical Properties of ADI and IADI Castings

Ahmed Negm[1], Samah Mohamed[2], Mervat Ibrahim[3], Ibrahim Moussa[2], Khaled Ibrahim[3]

[1]Modern Academy for Engineering and Technology, Cairo, Egypt
[2]Faculty of Engineering at Shoubra, Benha University, Cairo, Egypt
[3]Central Metallurgical Research and Development Institute, Cairo, Egypt
Email: anegm8747@gmail.com

How to cite this paper: Negm, A., Mohamed, S., Ibrahim, M., Moussa, I. and Ibrahim, K. (2021) Effect of Cast Thickness and Austenitizing Temperature on Microstructure and Mechanical Properties of ADI and IADI Castings. *Open Journal of Metal*, **11**, 21-35.
https://doi.org/10.4236/ojmetal.2021.113003

Received: August 11, 2021
Accepted: September 18, 2021
Published: September 21, 2021

Abstract

This investigation studies the impact strength, tensile strength, hardness, and wear behavior of thin wall austempered and intercritically austempered ductile iron samples with a chemical composition of 3.37% C, 2.7% Si, 0.30% Mn, 0.01% S, and 0.01% P. The austempered samples were austenitized at 900˚C for 1 h and rapidly quenched in a salt bath furnace at 375˚C for 1 h. The intercritically austempered samples were sub-austenitized at 810˚C for 1 h and rapidly quenched in a salt bath furnace at 375˚C for 1 h. The properties of the austempered and intercritically austempered thin wall plates of 5, 10, and 15 mm thickness were evaluated and compared to the as-cast samples. Austempering process affects greatly the tensile properties of all cast thicknesses where ultimate strength reached 1004 MPa for 5-mm thickness. Optimum impact toughness of 40 J was obtained for the austempered samples of 10- and 15-mm thicknesses. The intercritically austempered samples showed properties between the austempered and as-cast samples. Maximum wear resistance was also reported for the austempered samples due to containing retained austenite in the structure which in turn transformed into martensite that increases well the wear resistance. Maximum ultimate strength (1056) MPa and hardness (396 HV) were obtained for 5 mm ADI sample. Maximum impact toughness (43 J) was achieved for 15 mm IADI sample due to existing of pro-eutectoid ferrite in matrix. For all As-cast, ADI and IADI irons, wear resistance decreased with increasing sample thickness. Minimum wear rate (2.22×10^{-6} g/s) was reported for 5-mm ADI sample and maximum one (15.8×10^{-6} g/s) was registered for 15-mm as-cast DI sample, at a sliding speed of 2 m/s.

Keywords

DI, ADI, IADI, Retained Austenite, Wear Resistance

1. Introduction

Austempering is a heat treatment whereas the bainitic ferrite is generated during isothermal transformation of austenite at temperatures below the bainite-start (Bs) temperature. The phase, chemical composition, and heat treatment variations make it possible to produce a family of austempered ductile iron ADIs [1] [2] [3] [4] [5]. When heating ductile iron to an austenitizing temperature between the A1 and *a*T temperatures where (*a*) ferrite and austenite co-exist followed by subsequent austempering a unique mixed microstructure is formed that consists of pro-eutectoid ferrite, bainitic ferrite and carbon enriched austenite improving the machinability and ductility of the ductile iron. The resultant ductile iron from this process is the intercritically Austempered ductile iron (IADI) [6] [7] [8]. The proper heating temperature selected for heat treatments requiring full austenitizing is above the upper critical temperature and within the austenite + graphite. When the austenitizing temperature is too low, the pre-eutectoid coarse ferrite remains in the state of equilibrium with austenite and graphite so, it will not be a complete austenitizing treatment, regardless of the holding time [9] [10]. In 1989 Hayes *et al.* [11], invented an improved ductile iron by austempering which is called austempered ductile iron, since this history a lot of studies was carried out to get the best properties using the proper austempering on ductile iron. Investigations were done on the effect of austempering temperature, austempering time, and thickness on the mechanical properties, wear properties, microstructural features, fracture toughness, corrosion resistance and energy consumption [12]-[20].

After these all investigations the effect of both austempering and intercritically austempering with the change in the thickness up to small thicknesses of ductile iron still uncovered as well. The main purpose of this work is to get a new austempered ductile iron with better wear and mechanical properties that can be used for thin wall castings with the use of the proper heat treatment and casting thickness. Mechanical properties and microstructural examinations are performed to study the effect of different heat treatment parameters on thin wall ADI and IADI mechanical properties.

2. Experimental Work

Table 1 shows the chemical composition of the iron studied, which was casted, heat treated, and tested in the central metallurgical research and development institute in Cairo, Egypt. The molten metal was subjected to inoculation and Mg-treatment processes by adding Fe-Si inoculants and Fe-Si-Mg. The molten metal was poured at 1350˚C into molds with a superheat temperature of around

50˚C to ensure that the thin wall castings were optimally filled. The cast molds were composed of green silica sand with a content of 65 AFS grain fineness number which measures of the average size of the particles in a sand sample, 8% clay and 3.5% moisture content. For varying solidification rates, DI samples had variable geometry thicknesses. Casting design of the cast DI with different thicknesses is shown in Figure 1.

ADI samples with thicknesses of 5, 10 and 15 mm, were fully austenitized for 1 hour at 900˚C. Therefore, the samples were austempered in a salt bath of 50% KNO3 + 50% NaNO3 at 375˚C for 1 hour. IADI samples were austenitized at 810˚C, below the upper critical temperature, for 1 hour and then rapidly quenched into a salt bath at 375˚C for 1 hour (Figure 2).

Samples have been ground, polished, and chemically etched with a 2 Vol percent nital solution following the standard metallographic procedure for microstructural examination. The microstructure was studied using an optical microscope equipped with a digital camera. X-ray crystallography (model X' PERT PRO) was used to identify as-cast and heat-treated sample phases utilizing CU Kα X-ray source.

Table 1. Chemical composition of DI samples.

Fe	C	Si	Mn	P	S	Cr	Mo	Ni	Al	Cu	Mg
92.6	3.37	2.7	0.306	0.0136	0.0181	0.124	0.0857	0.164	0.017	0.467	0.0371

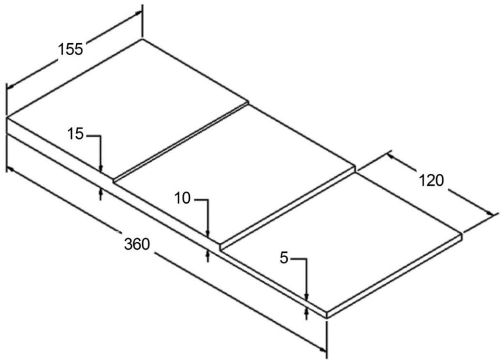

Figure 1. Layout of the as cast sample and their casting design.

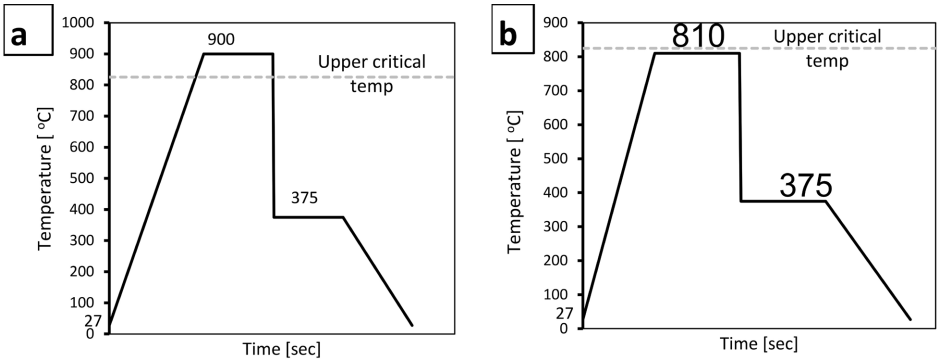

Figure 2. Charts illustrating the heat treatment typical temperature and time; (a) heat treatment of ADI, and (b) heat treatment of IADI.

A tensile test for as-cast, ADI and IADI samples were achieved at a constant displacement rate of 0.5 mm/min at room temperature by using a universal testing machine (Shimadzu) with a maximum capacity of 1000 KN. The dimensions corresponding to ASTM E8 were machined with rectangular tensile samples in 6 × 6 mm cross-section. A universal testing machine was used for the test. For each condition, at least four valid tests have been performed. Tensile properties were determined for each specimen, including yield strength, ultimate tensile strength and percentage elongation.

Hardness was measured on Vickers hardness device (Indentec) scale with 30 kg load and a diamond pyramid indentor typical for this scale. The hardness value was determined by the average of five measurements. The un-notched impact specimens (10 × 10 × 55 mm) were machined according to standard ASTM E23-98 specifications. The impact toughness value was determined by the mean of three measurements on the (Amslar) impact toughness machine with a maximum capacity of 150 J at room temperature. Wear rate was measured by using pin on disk wear testing machine. Wear rate was measured at four different disk speed values (0.5, 1, 1.5, 2) m/s.

3. Results and Discussion

3.1. Microstructure Investigation

The as-cast microstructure of the tested alloy in various wall thicknesses is shown in **Figure 3**. Of course, the cooling rate and consequently iron structure (the graphite nodule counts and metal matrix) are affected by varying wall thicknesses. The structure shows a white halo around the graphite nodules in a pearlite-ferrite matrix. The microstructure also demonstrates that increasing the wall thickness (decreasing the cooling rate) affects the graphite nodule's count, which is considered as an important factor in forming the iron matrix, **Table 2**. Volume fractions in **Table 2** are calculated with image analysis software. It is apparent that as the wall thickness decreased, the number of nodules count increased with forming more fine graphite size compared with thick section, **Figure 3(a)**. Moreover, increasing wall thickness resulted in a significant reduction in cooling rate which significantly increased the ferrite fraction in matrix [21].

Figure 4 shows the microstructure of the samples austenitized at 900˚C and austempered at 375˚C with different wall thickness. The microstructure composed of graphite spheroids dispersed in a matrix of ferritic needles and high carbon austenite called ausferrite. In this figure, the bainitic ferrite appears as dark needles, while austenite is the white phase between the bainitic ferrite needles. The ferrite needles normally nucleate and grow out of the austenite; matrix carbon is rejected in the remaining austenite, and the latter gets richer in carbon. The first austempering reaction in which the austenite decomposed into ferrite and high carbon austenite goes slow down at thick wall sections and thus requires long time for transformation completion. Also, wall thickness has an effect on morphology and fineness of the bainitic ferrite that are formed at austempering temperature of 375˚C.

Table 2. The results of metallographic measurements of the samples investigated.

	Thickness	Nodules count/mm^2	Microstructural constituents (volume %)		
	[mm]		Graphite	ferrite	pearlite
As-cast	5	420	10.7	10.2	79.3
	10	360	10.9	15.3	74.1
	15	255	11.9	18.2	70.1

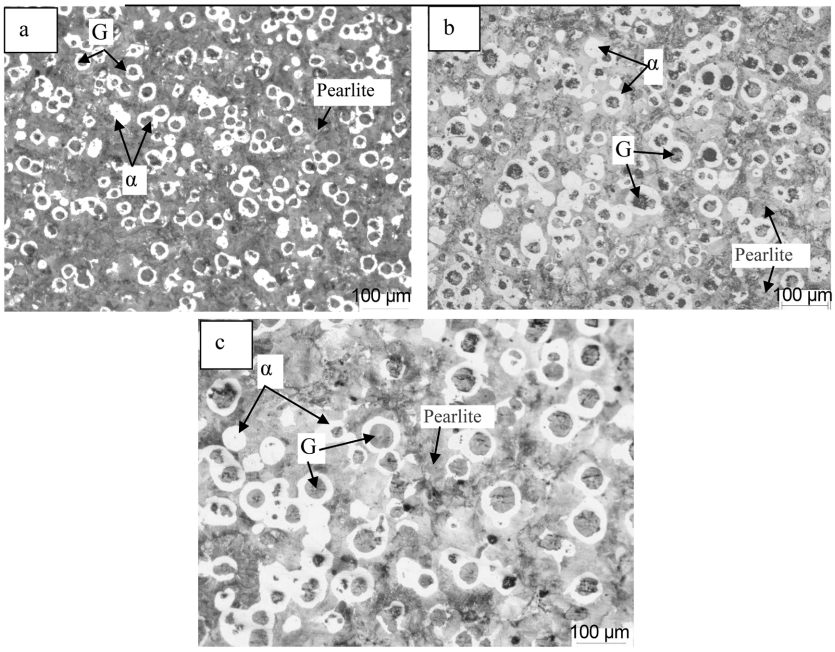

Figure 3. Microstructure of as cast DI samples with different thicknesses (a) 5 mm, (b) 10 mm, and (c) 15 mm (*α*: ferrite, G: graphite).

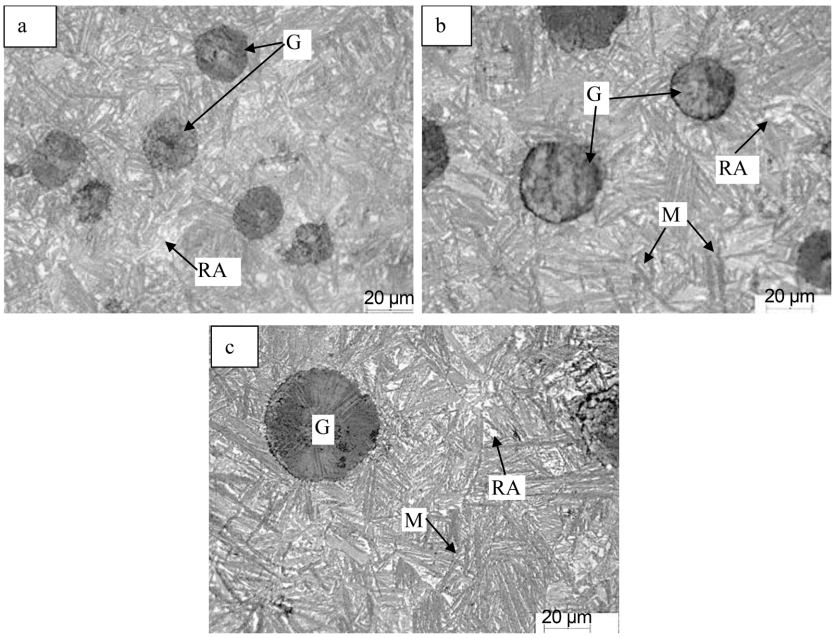

Figure 4. Microstructure of ADI specimens (a) 5 mm thickness, (b) 10 mm thickness, and (c) 15 mm thickness (RA: retained austenite).

Figures 4(a)-(c) show the developed microstructure after two hours of austenitizing and austempering treatments for DI with various wall thicknesses. The austempering treatment of a 5 mm thin section resulted in complete transformation of austenite into a fine ausferrite matrix with little amount of retained austenite, as shown in Figure 4(a). At thinner sections, high nodule counts were dispersed in the matrix and more ferrite needles nucleate around them and hence promote fine ausferritic matrix, Table 3. In contrast, more blocky volumes of austenite are retained by increasing wall thickness, which would likely transform to martensite on cooling to room temperature, Figure 4(c). These microstructure observations are confirmed by XRD analysis, as shown in Figure 5, where peaks intensity for austenite phase decreased with decreasing wall thickness.

Microstructures of intercritically austempered samples with various wall thicknesses and austempered at 375˚C are shown in Figure 6. Ausferrite (dark areas) and proeutectoid ferrite (white areas) formed in the matrix around graphite nodules in the microstructure. It was observed that the austenite started to nucleate at eutectic cells where manganese segregated at these regions. Manganese is an austenite stabilizing element and favors nucleation of austenite in these regions. However, areas surrounding the graphite nodules were mostly ferritic. This is related to the segregation of silicon which is a ferrite stabilizer element during solidification process around the graphite nodules.

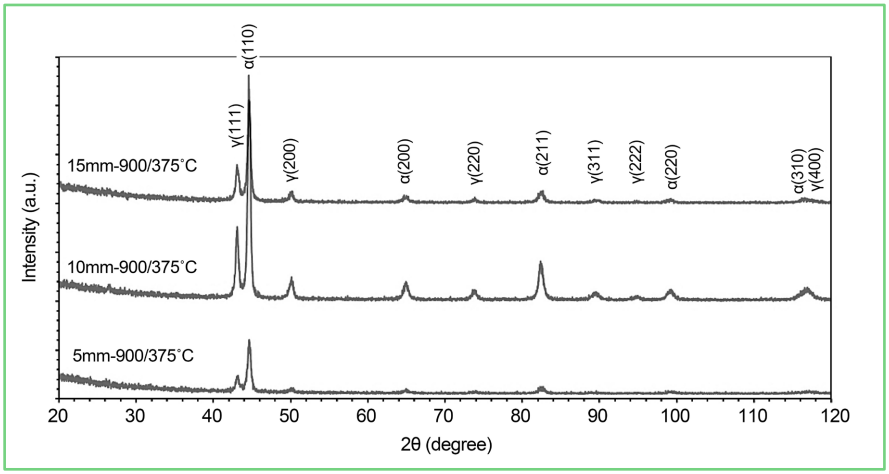

Figure 5. XRD analysis for ADI samples austenitized at 900˚C and austempered at 375˚C.

Table 3. The results of metallographic measurements of ADI and IADI samples.

	Thickness [mm]	Nodules count/ mm^2	Microstructural constituents (volume %)				
			Graphite	Proeutectoid ferrite	Bainitic ferrite	High carbon austenite	Ausferrite
ADI	5	412	9.6	-	73.3	17.3	90.6
	10	314	9.5	-	65.8	25.2	91.0
	15	248	11.4	-	68.8	20.1	88.9
IADI	5	440	11.2	27.3	48.8	12.9	61.7
	10	262	10.8	35.7	45.3	10.0	53.3
	15	269	13.4	42.7	29.0	15.2	44.2

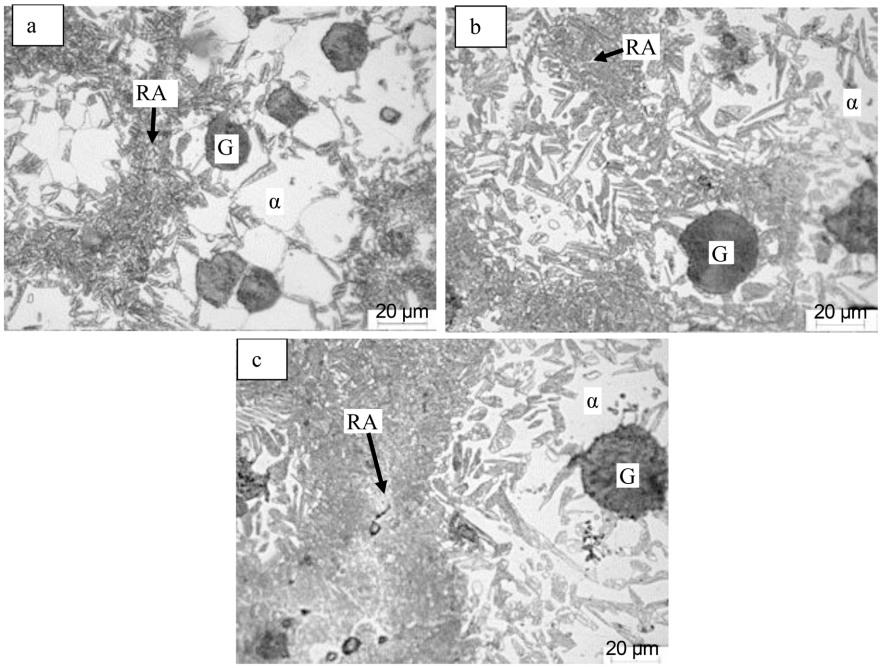

Figure 6. Microstructure of IADI specimens (a) 5 mm thickness, (b) 10 mm thickness, and (c) 15 mm thickness (RA: retained austenite & *α*: pro-eutectoid ferrite).

The effect of wall thickness on the volume fraction of pro-eutectoid ferrite and ausferrite is also shown in **Figure 6**. **Table 3** shows that decreasing wall thickness leads to a decrease in the volume fraction of proeutectoid ferrite, while increasing the volume fraction of ausferrite. This is due to the presence of higher amounts of pearlite in the as-cast structure at a thin section of 5 mm, which promotes the formation of austenite during heating at 810˚C and decreases the ferrite volume percent. During holding at the isothermal temperature of 375˚C, the high temperature austenite is transformed to ausferrite. In addition, higher cooling rate of thin sections leads to an enhanced nucleation and refined the ausferrite structure. On the other hand, at thick sections of 15 mm, the diffusivity of carbon increases which in turn enhances the growth of ferrite needles and high carbon austenite resulting in a course ausferrite structures. The volume fraction of austenite in the ausferrite was determined by X-ray analysis technique, **Figure 7**. It was observed that the volume fraction of retained austenite at thin wall section was low compared to thick section, where the peaks intensity of the austenite phase decreases with decreasing the wall thickness. As mentioned earlier, the volume fraction of retained austenite considerably increases with increasing wall thickness.

3.2. Mechanical Properties

The mechanical properties of the tested samples are given in **Table 4**. Variation of mechanical properties with wall thickness depended on nature and amount of phases presented in each heat treatment condition as well as as-cast sample.

Additionally, the variation of strength as a function of wall thickness for as-cast,

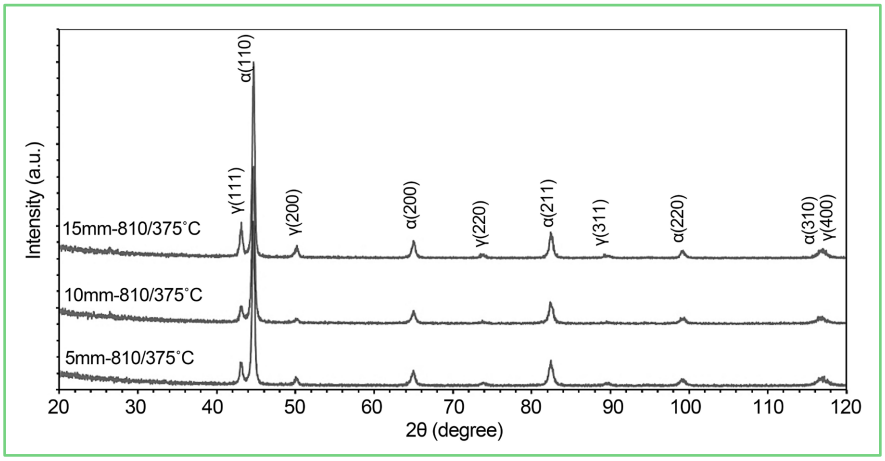

Figure 7. XRD analysis for ADI samples austenitized at 810˚C and austempered at 375˚C.

Table 4. Mechanical properties for the tested samples.

Heat treatment [˚C]	Thickness [mm]	Ultimate strength [MPa]	Yield Strength [MPa]	%Elongation	Impact strength [J]	Hardness HV
As-cast	5	675	620	7.9	11	280
As-cast	10	674	615	8	28	260
As-cast	15	660	600	10	29	250
900/375	5	1056	996	3.7	31	396
900/375	10	1006	927	4.9	32	351
900/375	15	963	950	4	37	331
810/375	5	896	849	6.8	34	344
810/375	10	867	707	6.7	40	317
810/375	15	746	650	6.6	43	298

ADI and IADI are presented in **Figure 8** & **Figure 9**. The highest ultimate and yield strength were obtained for ADI samples and the lowest ones were reported to as-cast samples. The strength of dual structures (IADI samples) lies between as-cast and ADI samples. For austempered and as-cast samples, ultimate and yield strengths registered the highest values for thin wall thickness of 5 mm. This is related to the decrease in the volume fraction of proeutectoid ferrite in IADI and refining of ausferritic structures with lower amounts of retained austenite in ADI at thinner wall thickness. The highest values of ultimate and yield strengths which obtained for ADI samples could be related to the reinforcing effect of ausferrite in the structure.

These high-strength values were associated of course with low elongation values. **Figure 10** illustrates that the highest values of elongation were reported for the as-cast samples and then for IADI samples compared with ADI ones. It was obvious that the presence of ferrite in as-cast condition especially at thick section and proeutectoid ferrite at (IADI) resulted in a noticeable increase at the elongation values.

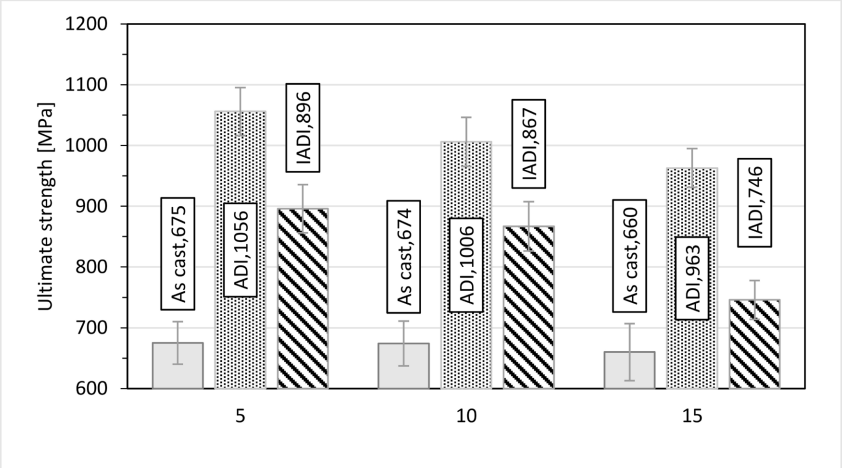

Figure 8. The variation of ultimate strength as a function of wall thickness for as-cast, ADI, and IADI.

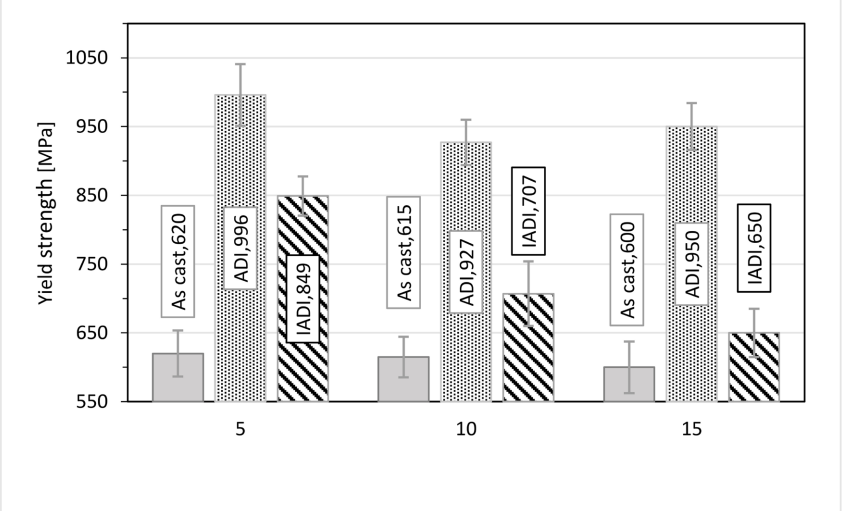

Figure 9. Variation of yield strength vs. wall thickness for as-cast, ADI, and IADI.

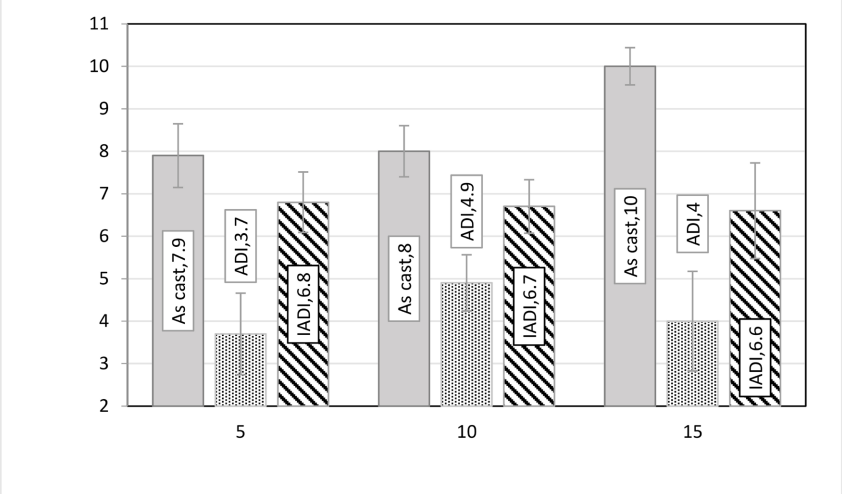

Figure 10. The variation of %Elongation vs. wall thickness for as-cast, ADI, and IADI.

Hardness of austempered and as-cast samples was measured at different cross sections, Figure 11. Hardness had the same trend of ultimate and yield strength where it decreased with increasing wall thickness and the highest values were obtained in case of ADI samples. This is attributed to its unique microstructure of ausferritic matrix which refined by decreasing the wall thickness and consequently hardness increased. Hardness decreased slightly in case of dual phase IADI samples comparing with conventional ADI due to presence of proeutectoid ferrite besides ausferrite. The as-cast condition registered the lowest hardness values due to its microstructure which composed of pearlite and ferrite.

Figure 12 shows the effect of wall thickness on impact toughness of austempered (ADI & IADI) and as-cast conditions. It can be seen that as-cast samples indicated the smallest value of toughness for all cross sections comparing to that heat-treated samples. In addition, a sharp drop in impact toughness was observed for as-cast condition especially for thin wall thickness of 5 mm. This is related to the high amount of pearlite phase especially in thin section which is considered as brittle phase. In contrast, IADI samples show the highest value of impact toughness whereas ADI samples lie between the as-cast and IADI conditions. Additionally, for all studied conditions, the values of impact toughness increased with increasing wall thickness. Hence, it can be concluded that the variation in impact toughness is attributed to the type and volume percent of present phases in the microstructure.

As-cast, ADI, and IADI specimens were submitted to a wear test where the sliding speed was increased from 0.5 to 2 m/s. As-cast samples wear rate ranged between 7.1×10^{-6} to 15.8×10^{-6} g/s (Figure 13). Wear rate increased with increasing wall thickness. 5-mm samples had the lowest wear rate in all cases; this was because it had a comparably high cooling rate giving higher amounts of pearlite and lower pearlite spacing. Figure 14 shows that increasing percentage

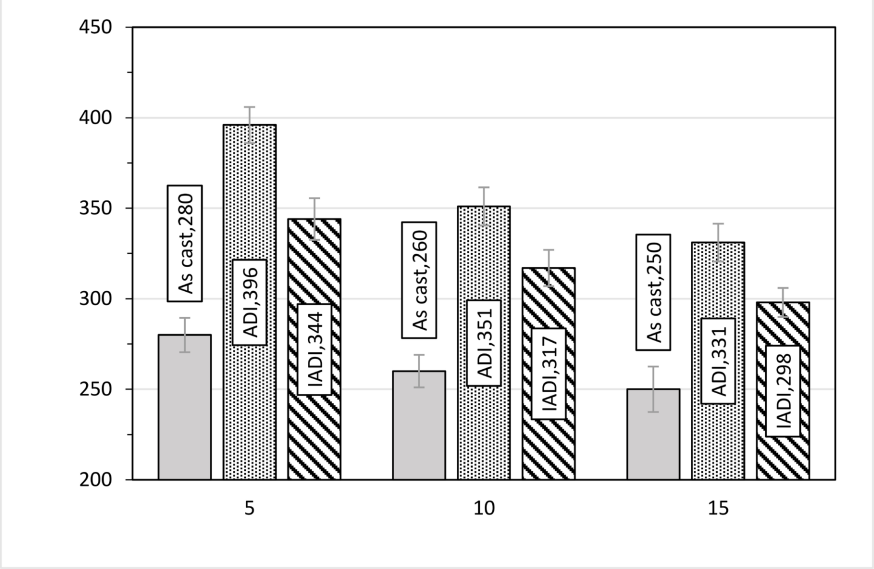

Figure 11. The variation of Hardness as a function of wall thickness for as-cast, ADI, and IADI.

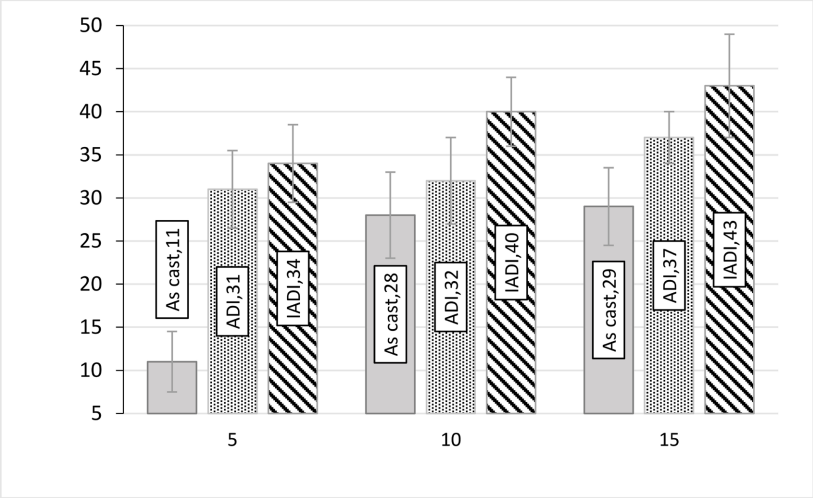

Figure 12. The variation of Impact toughness as a function of wall thickness for as-cast, ADI, and IADI.

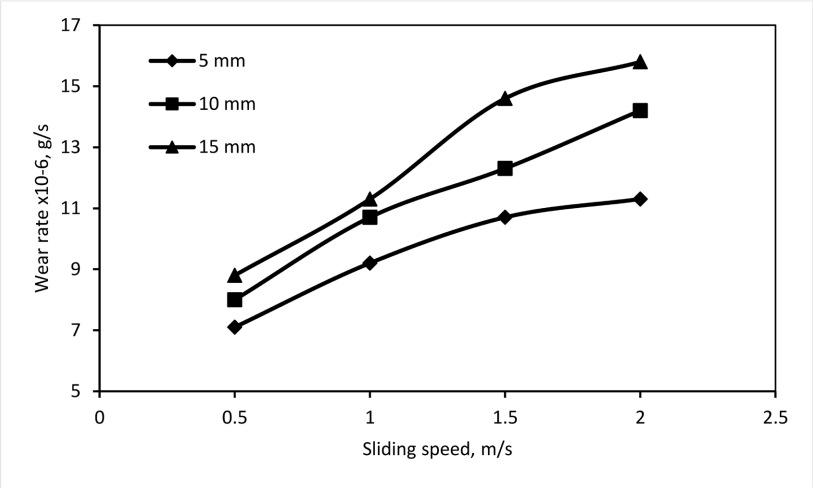

Figure 13. The variation of wear rate as a function of sliding speed for as-cast samples.

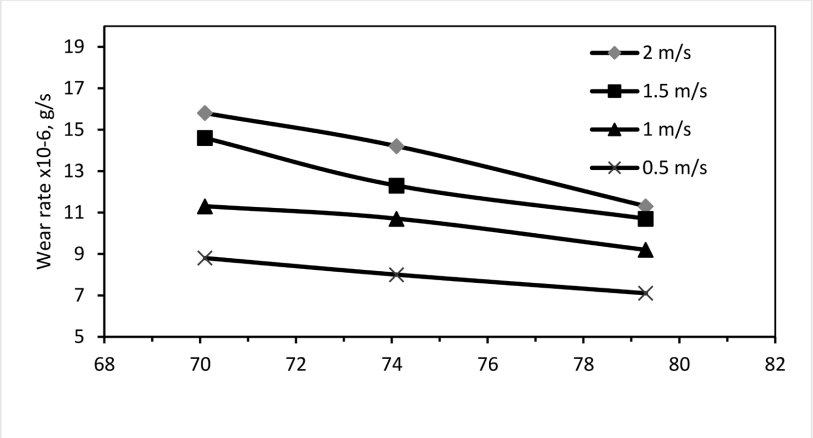

Figure 14. The variation of wear rate as a function of %pearlite for as-cast samples at different sliding speeds.

of pearlite improves dramatically As-cast DI wear resistance. Figure 15 shows that ADI samples reported the best wear resistance. For small sliding speed 0.5 and 1 m/s, ADI samples wear rate changed slowly, then the 10-mm and 15-mm samples wear rate got increased rapidly at 1.5 and 2 m/s speeds. 5-mm samples wear rates below 1.5 m/s speed changed slowly. Finer ferrite needles with higher volume fraction of austenite and martensite in the ADI matrix influenced the wear behavior of ADI. ADI samples at 2 m/s sliding speed had wear rate about 42% that of As-cast ones. IADI samples having a coarser pro-eutectoid ferrite and lower amount of retained austenite reported an intermediate wear rate between As-cast and ADI samples, Figure 16. Normally, samples that have high hardness numbers reported lower wear rates. Figure 17 shows that wear rate decreases with the increase in hardness for all samples, this result agrees with that reported by Vélez [22].

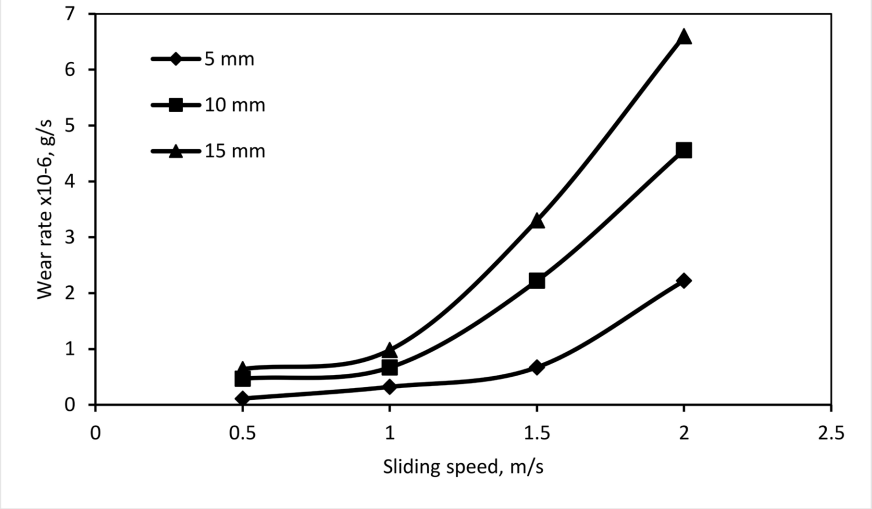

Figure 15. The variation of wear rate as a function of sliding speed for ADI samples.

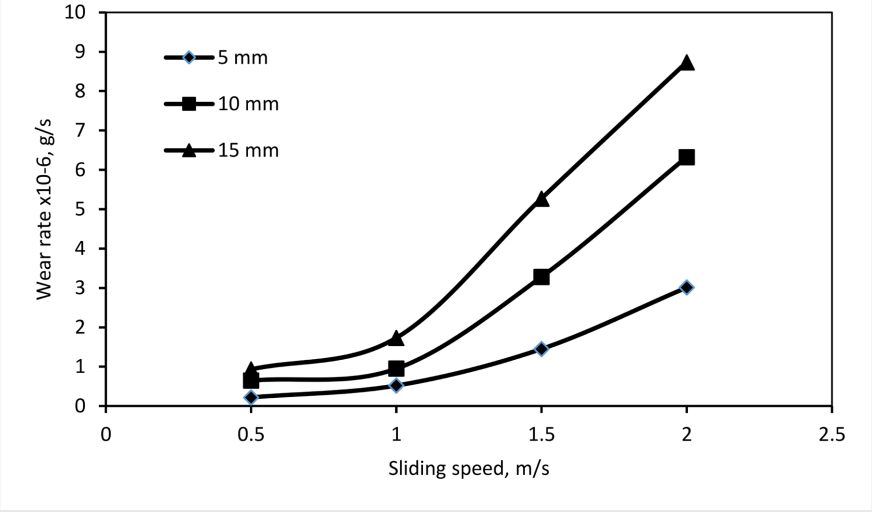

Figure 16. The variation of wear rate as a function of sliding speed for IADI samples.

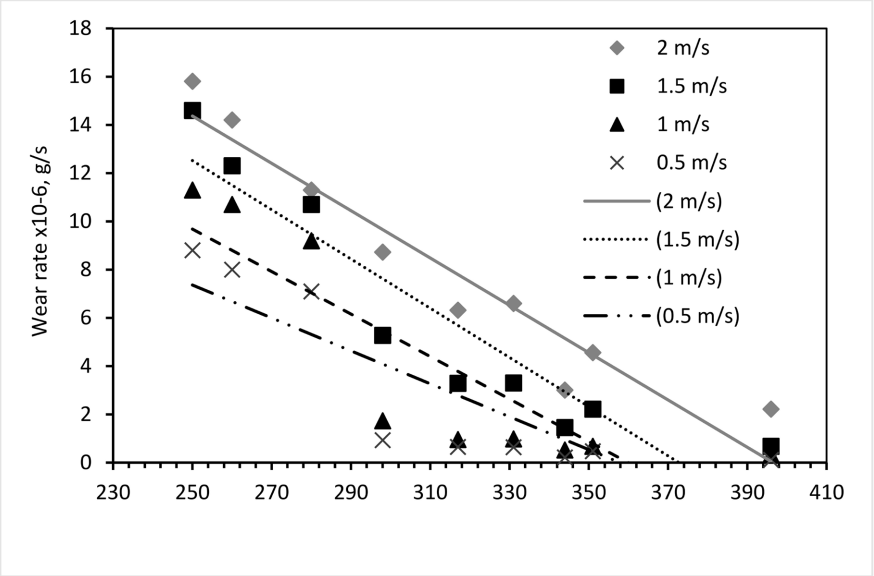

Figure 17. The variation of wear rate as a function of hardness for ADI samples at different sliding speeds.

4. Conclusion

In this work, the microstructures, wear, and mechanical properties of two different austempering techniques as well as the as-cast condition were investigated as function of wall thickness. The following conclusions can be concluded below:

- Wall thickness has a pronounced effect on the matrix structure and graphite nodule count. Where, in as-cast condition, decreasing wall thickness resulted in a significant increase in graphite nodule counts and pearlite fraction in the matrix.
- The microstructure of ADI is composed of ausferrite and retained austenite, while IADI matrix consists of ausferrite and polygonal ferrite. In addition, decreasing wall thickness leads to finer ausferrite structure in both austempering techniques.
- Maximum ultimate strength, yield strength, wear resistance, and hardness were obtained for ADI samples. In addition, the highest value of tensile strengths, wear resistance, and hardness was reported to the thinner wall thickness of 5-mm in all conditions (as-cast, ADI, and IADI).
- Impact toughness increased with increasing wall thickness for all samples. IADI of 15-mm sample obtained maximum impact toughness of 43 J, while minimum impact (11 J) was reported for 5-mm as-cast sample.

Conflicts of Interest

The authors declare no conflicts of interest regarding the publication of this paper.

References

[1] Soliman, M., Nofal, A. and Palkowski, H. (2020) Effect of Thermo-Mechanical

Processing on Structure and Properties of Dual-Phase Matrix ADI with Different Si-Contents. *International Journal of Metalcasting*, **14**, 853-860. https://doi.org/10.1007/s40962-020-00477-4

[2] Guesser, W.L., Lopes, C.L. and Bernardini, P.A.N. (2020) Austempered Ductile Iron with Dual Microstructures: Effect of Initial Microstructure on the Austenitizing Process. *International Journal of Metalcasting*, **14**, 717-727. https://doi.org/10.1007/s40962-019-00397-y

[3] Uyar, A., Sahin, O., Nalcaci, B. and Kilicli, V. (2021) Effect of Austempering Times on the Microstructures and Mechanical Properties of Dual-Matrix Structure Austempered Ductile Iron (DMS-ADI). *International Journal of Metalcasting*. https://doi.org/10.1007/s40962-021-00617-4

[4] Janowak, J.F. and Norton, P.A. (1985) A Guide to Mechanical Properties Possible by Austempering, 1 Spercent Ni, 0.3 Percent Mo Iron. *AFS Transactions*, **88**, 123-135.

[5] Janowak, J.F., Gundlach, R.B., Eldis, G.T. and Rohrting, K. (1982) Technical Advances in Cast Iron Metallurgy. *International Cast Metal Journal*, **6**, 28-42.

[6] Kobayashi, T. and Yamada, S. (1996) Effect of Holding Time in the (α + γ) Temperature Range on Toughness of Specially Austempered Ductile Iron. *Metallurgical and Materials Transactions A*, **27**, 1961-1971. https://doi.org/10.1007/BF02651945

[7] Cerah, M., Kocatepe, K. and Erdogan, M. (2005) Influence of Martensite Volume Fraction and Tempering Time on Tensile Properties of Partially Austenitized in the (α + γ) Temperature Range and Quenched + Tempered Ferritic Ductile Iron. *Journal of Materials Science*, **40**, 3453-3459. https://doi.org/10.1007/s10853-005-0415-3

[8] Machado, H.D., Aristizabal-Sierra, R., Garcia-Mateo, C. and Toda-Caraballo, I. (2020) Effect of the Starting Microstructure in the Formation of Austenite at the Intercritical Range in Ductile Iron Alloyed with Nickel and Copper. *International Journal of Metalcasting*, **14**, 836-845. https://doi.org/10.1007/s40962-020-00450-1

[9] Galarreta, I.A., Boeri, R.E. and Sikora, J.A. (1997) Free Ferrite in Pearlitic Ductile Iron—Morphology and Its Influence on Mechanical Properties. *International Journal of Cast Metals Research*, **9**, 353-358. https://doi.org/10.1080/13640461.1997.11819677

[10] Kowalski, A., Kluska-Nawarecka, S. and Regulski, K. (2013) ADI after Austenitising from Intercritical Temperature. *Archives of Foundry Engineering*, **13**, 81-88. https://doi.org/10.2478/afe-2013-0016

[11] Hayes, W.J., Martrone, H.A. and Johnson, P.D. (1989) Process of Making an Austempered Ductle Ron Article. Academic Press, San Diego.

[12] Panneerselvam, S., Martis, C.J., Putatunda, S.K. and Boileau, J.M. (2015) An Investigation on the Stability of Austenite in Austempered Ductile Cast Iron (ADI). *Materials Science and Engineering*: *A*, **626**, 237-246. https://doi.org/10.1016/j.msea.2014.12.038

[13] Vechet, S., Kohout, J. and Klakurkova, L. (2008) Fatigue Properties of Austempered Ductile Iron in Dependence on Transformation Temperature. *Materials Science*, **14**, 324-327.

[14] Ovali, I., Kilicli, V. and Erdogan, M. (2013) Effect of Microstructure on Fatigue Strength of Intercritically Austenitized and Austempered Ductile Irons with Dual Matrix Structures. *ISIJ International*, **53**, 375-381. https://doi.org/10.2355/isijinternational.53.375

[15] Sellamuthu, P., Samuel, D.G. H., Dinakaran, D., Premkumar, V.P., Li, Z. and Seetharaman, S. (2018) Austempered Ductile Iron (ADI): Influence of Austempering Temperature on Microstructure, Mechanical and Wear Properties and Energy

Consumption. *Metals*, **8**, Article No. 53. https://doi.org/10.3390/met8010053

[16] Putatunda, S.K., Panneerselvam, S. and Alshwigi, M. (2015) Development of Nanostructured Austempered Ductile Cast Iron (ADI). 2*8th Heat Treating Society Conference*, Detroit, 20-22 October 2015, 71-75.

[17] Cardoso, P.H. S., Israel, C.L. and Strohaecker, T.R. (2014) Abrasive Wear in Austempered Ductile Irons: A Comparison with White Cast Irons. *Wear*, **313**, 29-33. https://doi.org/10.1016/j.wear.2014.02.009

[18] Rocha-Reséndez, R. and Calderon, F.A. (2018) Corrosion Behavior of Austempered Ductile Iron Used in the Aeronautical Industry Evaluated on Acid Solutions. *International Materials Research Congress* 2016, Cancún, 14-19 August 2016, 73-82. https://doi.org/10.1007/978-3-319-65611-3_7

[19] Aristizabal, R., Foley, R., Griffin, J. and Monroe, C. (2014) Austemperability of Intercritically Austempered Ductile Iron (IADI). *AFS Transactions*, **3**, 279-286.

[20] Gundlach, R. and Boileau, J. (2017) Influence of Intercritical Austempering on the Microstructure and Mechanical Properties of Ausempered Ductile Iron (ADI). *Materials Science and Engineering*: *A*, **694**, 72-80. https://doi.org/10.1016/j.msea.2017.03.096

[21] Górny, M. and Tyrała, E. (2013) Effect of Cooling Rate on Microstructure and Mechanical Properties of Thin-Walled Ductile Iron Castings. *Journal of Materials Engineering and Performance*, **22**, 300-305. https://doi.org/10.1007/s11665-012-0233-0

[22] Vélez, J.M., Tanaka, D.K., Sinatora, A. and Tschiptschin, A.P. (2001) Evaluation of Abrasive Wear of Ductile Cast Iron in a Single Pass Pendulum Device. *Wear*, **251**, 1315-1319. https://doi.org/10.1016/S0043-1648(01)00760-8